International Journal of Thermofluid Science and Technology (2023)
Volume 10, Issue 4, Paper No. 100403
https://doi.org/10.36963/IJTST.2023100403

Research Article

Evaluation of conventional fluid mechanic theory in small channels with singularity

Sid Ali Si Salah*, Abdelwahid Azzi, El Ghalia Filali

Faculty of Mechanical and Process Engineering, Houari Boumedienne University, B.P. 32 El Alia, Algiers, Algeria,

ATICLE INFO

Received: 15 Aug. 2023;
Received in revised form:
28 Sep. 2023;
Accepted: 18 Nov. 2023;
Published online:
30 Nov. 2023

Keywords:
microchannel
backward-facing step
Control Volume Finite Element Method (CVFEM)
expansion loss coefficient
friction factor

ABSTRACT

This study employs numerical simulations using the combined control volume finite element method (CVFEM) to analyze 2D steady, incompressible laminar flow over a microscale backward facing step within a horizontal duct. The investigation focuses on the impact of Reynolds number (Re_d) and expansion ratio (ER) on flow behavior, aiming to assess the applicability of conventional hydrodynamics at the microscale. The findings reveal that, for an expansion ratio of 2, the flow structure transforms progressively with varying Reynolds numbers in both laminar and transitional flow regimes. Notably, three recirculation zones develop downstream of the step, two along the lower wall and one along the upper wall. The primary recirculation zone's size expands as Reynolds number increases, contracting when a third recirculation zone emerges on the lower wall ($Re_d \geq 950$). The study successfully matches its numerical predictions with experimental observations from larger-scale backward-facing steps for Reynolds numbers up to 500, maintaining two-dimensional flow characteristics. Furthermore, the computed velocity profiles align closely with experimental outcomes, except for Re_d = 1000, where the experimental flow shifts to three-dimensionality. The study also examines loss coefficients (Ke), revealing substantially higher values than conventional macro systems for Reynolds numbers above 200. However, for lower Reynolds numbers, the loss coefficient varies accordingly. For expansion ratios of 1.5, 2.0, and 2.5, fluid flow properties such as pressure, Poiseuille number, and friction factors exhibit good agreement with macroscale theory for fully developed laminar flow ($Re_d \leq 500$).

1. Introduction

The importance of flow in microchannels and micro-devices lies in the rapid progress of Micro-Electro-Mechanical Systems (MEMS). These micro-channels are of great importance in cooling micro-electronic devices [1]. micro heat exchangers [2-4], micro combustion chambers [5-6], bioengineering, biomedical instruments, small-sized refrigeration systems, etc. Fluid flows through sudden expansion and contraction

*Corresponding e-mail: ssi-salah@usthb.dz (Sid Ali Si Salah)

Nomenclature

C_f	the skin friction coefficient	*Xo*	outet microchannel length, m
d	hydraulic diameter, m	*x*	axial coordinate, m
ER	expansion rate	*y*	Transversal coordinate, m
h	microchannel inlet height, m		
H	microchannel outlet height, m	*Greek symbols*	
$\vec{J}$	total flux (diffusion convection)	ρ	density, kg/m^3
K	the singular pressure drop coefficient	μ	dynamic viscosity, *kg/m. s*
Po	Poiseuille number	ϕ	mass flow parameter, m·s$\sqrt{\text{K}}$
p	pressure, Pa		
Re	Reynolds number		
S	step height, m	*Subscripts*	
Sø	source term	0	turbine inlet
u	Axial component of velocity, m/s	2	blade outlet
v	transversal component of velocity, m/s	*exp*	experimental
U	inlet velocity, m/s	*pred*	predicted
Xe	inlet microchannel length, m	*ref*	value at the reference point

engine components, such as flow in diffusers [7], airfoils, combustion chambers [8], heat exchangers and solar collector [9]. Almost all previous works have focussed essentially on a conventional channel with sudden enlarging and contraction.

Armaly et al. [10] realized an experimental investigation focusing on the flow over a backward-facing step (BFS) at various Reynolds numbers (Re_d). The study covered laminar (Re_d < 1200), transition (1200 < Re_d < 6600), and turbulent (Re_d > 6600) regimes. The researchers utilized Laser-Doppler measurements to analyze the velocity distribution and reattachment length downstream of a single BFS placed within a two-dimensional channel with an expansion ratio of ER=2. Their findings revealed that the presence of the step induced a depression in the flow, leading to its separation into distinct zones. Notably, three recirculation zones emerged behind the step. When the Reynolds number was less than 400, a recirculation zone was observed near the step itself. However, for Reynolds numbers greater than 400, an additional secondary recirculation zone formed at the top wall, originating close to the position where the primary recirculation ended. For the transitional

range of Reynolds numbers (1200 ≤ Re_d < 6600), the length of the primary recirculation zone decreased, and a new vortex emerged at the bottom wall. This trend of behavior was consistent with the outcomes reported by Gartling et al. [11] and Lee et al. [12].

Hammad and al [13] employed Particle Image Velocimetry (PIV) as a technique in their experimental investigation to visualize the flow dynamics within an axisymmetric sudden expansion. Their study revealed distinct features within the flow, notably illustrating the occurrences of separation, reattachment, and recirculation. Notably, they successfully established a relationship between key parameters, including reattachment lengths, redevelopment length, and the strength of the recirculation vortex, with variations in Reynolds number. This correlation sheds light on the influence of Reynolds number on these flow characteristics, providing valuable insights into the behavior of the flow through an axisymmetric sudden expansion.

In their study, Lima et al. [14] conducted numerical investigations of fluid flow through a (BFS) across a Reynolds number range of 100 to 2500. At lower Reynolds numbers, characterized

by a single recirculation zone in the flow, their numerical findings were consistent with prior experimental work by Armaly et al. [10]. However, as the Reynolds number increased, leading to the emergence of a third vortex and a transition from laminar to turbulent flow, the impact on the results was inexplicable. The study demonstrated agreement between numerical

simulations and experiments for the single recirculation zone regime, yet encountered challenges in comprehending the effects of the laminar-to-turbulent transition at higher Reynolds numbers. This emphasizes the need for further research to elucidate and model the complexities of this flow phenomenon.

Roy et al. [15] conducted a study on turbulent airflow within an axisymmetric enlargement. They observed that turbulence levels increased downstream of the expansion section, attributed to the sudden geometric change. In the turbulent flow regime, they noted that higher Reynolds numbers and smaller expansion ratios led to a reduction in both reattachment length (where the flow reattaches after separation) and recirculation strength. This suggests that as Reynolds numbers increased and expansion ratios decreased, the turbulent flow exhibited a shorter reattachment length and weaker recirculation. Sudipta et al. [16] carried out a numerical analysis of fluid flow involving sudden expansion and contraction. Their findings revealed that both the Reynolds number and the expansion/contraction ratio play significant roles in shaping the flow characteristics. Specifically, the size of the recirculation zone, the length at which the flow reattaches after separation, and the process of flow redevelopment were all influenced by these factors. Higher expansion ratios coupled with lower Reynolds numbers led to flow structures becoming unstable. Ultimately, the study concluded that the dimension of the recirculation zone, the reattachment length of the flow, and the redevelopment of the flow were individually impacted by the Reynolds number and the expansion/contraction ratio. In their study, Nowruzi et al. [17] conducted a stability analysis of a 2-D laminar backward-facing step (BFS) flow. They investigated this flow under different conditions of expansion ratios and Reynolds numbers. Their findings revealed that as the expansion ratio increases, the flow becomes unstable. This suggests that changes in the geometric configuration, particularly the expansion ratio, have a significant impact on the stability characteristics of the laminar backward-facing step flow.

Research on microscale sudden expansion and contraction phenomena has been explored. Toufik Chalfi and al. [18] conducted experimental investigations using water flow in microchannels with expansion and contraction features, employing two different diameters (0.84 mm and 1.6 mm). Notably, they observed that in laminar flow conditions, expansion loss coefficients substantially increased with rising Reynolds numbers. However, the values of the contraction loss coefficient aligned with classical predictions from channel flow theory. Similar findings were also reported by Abdelall et al. [19]. These studies collectively suggest that expansion and contraction effects exhibit distinctive behavior in microchannels, where expansion loss coefficients respond to Reynolds numbers differently compared to the contraction loss coefficients, which remain consistent with classical theoretical expectations.

Hang et al. [20] performed an experimental investigation focused on both laminar and turbulent flows within a micro pipe featuring a contraction, with the primary aim of assessing the resulting pressure drop. The experimentation employed deionized water at typical environmental conditions of temperature and pressure. The study was executed across three distinct test sections characterized by area ratios (σ, the ratio of downstream area to upstream area) of 0.284 and 0.274. The study's key findings include the recognition that conventional correlations are inadequate for predicting the contraction coefficient in turbulent flow scenarios. Moreover, the research observed a trend wherein the coefficient of contraction (Kc) exhibited a reduction as the Reynolds number and the outlet diameter of the micro pipe increased. Sepideh et al. [21] employed an advanced Particle Image Velocimetry (PIV) technique to visually study the flow characteristics within micro circular sudden expansions. Their research revealed a notable observation: up to a Reynolds number of 20, both the redevelopment length and the recirculation length exhibited a linear growth pattern with increasing Reynolds numbers and expansion ratios. This finding highlights a systematic relationship between these flow parameters and the Reynolds number and expansion ratio within the examined range. These findings are in accordance with the outcomes obtained by Hammad et al. [13] in

their study of conventional sudden expansion channels.

Hassnia et al. [22] carried out a comprehensive numerical investigation involving 2D and 3D simulations of laminar and turbulent flows within microchannels featuring sudden expansions. The finite element method was employed for this study. The microchannel expansion ratio was set at ER=3, and the Reynolds number range under investigation spanned from 0.1 to 40. The results of their research unveiled the emergence of a vortex immediately after the expansion section, particularly pronounced at low Reynolds numbers. Furthermore, the study demonstrated that as the Reynolds number increased, the size of this vortex grew, concomitantly leading to a decrease in the friction factor. This suggests that variations in Reynolds numbers significantly influence the flow patterns and characteristics within sudden expansion microchannels.

The literature presented highlights a notable disparity in the research focus between macro and micro sudden expansion and contraction phenomena. While numerous studies have been conducted on the macro scale, only a limited number of experimental and numerical investigations have been dedicated to understanding the flow behavior within microchannels featuring sudden expansion and contraction. This research gap is significant given the growing importance of microfluidic devices. Understanding the hydraulic characteristics of flows in microchannels with sudden expansion or contraction is crucial. Developing accurate correlations is essential for the precise design of microfluidic devices. These correlations serve as valuable tools for predicting and optimizing the behavior of fluids in microscale geometries, which have unique characteristics compared to their macro counterparts. The outcomes of such studies hold potential for enhancing the performance and efficiency of microfluidic systems, thus contributing to advancements in various fields reliant on microfluidics technology.This investigation explores the impact of varying Reynolds numbers and expansion ratios on the hydrodynamic characteristics of a two-dimensional laminar flow within a microscale backward-facing step (BFS) microchannel. To accomplish this, a Fortran-based code is developed, employing the Control Volume Finite Element Method, as referenced in [23-25]. The main goal is to assess the applicability of established patterns and relationships from conventional channels and determine their relevance when extended to the microscale domain.

2. Mathematical modeling

2.1 Geometry and governing equations

The physical domain, illustrated in Fig.1 is a microchannel with a backward-facing step. The enlarged section is maintained constant H=600 μm, contrary to the height of the inlet section which is variable. The length of the first microchannel Xe, is chosen to guarantee a fully developed flow before the singularity and the length Xo of the microchannel of height H, in manner that the outlet has no influence on the formation of the of recirculation zones. The considered expansion ratios are ER = H/h= 1.5; 2; and 2.5. Fig.1 also shows the recirculation regions (**I**, **II**, and **III**) and their detachment and reattachment abscises X_1, X_2, X_3, X_4, and X_5.
The following assumptions are used: (i) Newtonian and continuum fluid; (ii) two-dimensional, steady, incompressible, and laminar flow; (iii) continuous fluid properties; and (iv) with negligible external body forces.
Using ϕ , Γϕ , and Sø as the main variables of this study, in accordance with Table 1, the continuity and momentum equations can be written in the following generalized form:

$$\vec{\nabla}.\vec{J}_{\phi} = S_{\phi} \qquad (1)$$

with: $\vec{J}_{\phi} = \rho \vec{V}\ \phi - (\Gamma_{\phi})\ \vec{\nabla}\phi$

Table 1 Diffusivity coefficient expressions and source term

Equation	ϕ	Γ_{ϕ}	S_{ϕ}
Continuity	1	0	0
x- Momentum	*u*	μ	$-\frac{\partial P}{\partial x}$
y- Momentum	v	μ	$-\frac{\partial P}{\partial y}$

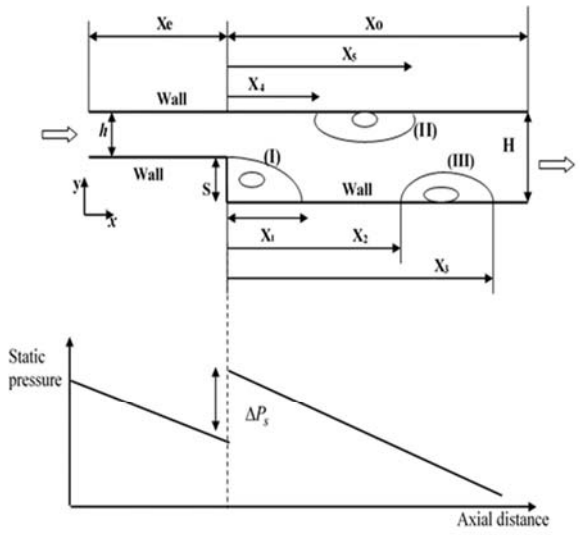

Height of the inlet microchannel (µm)	*h*	240,300,400
Height of the outlet microchannel (µm)	*H*	600
Inlet microchannel length(mm)	X_e	10, 12, 27
Outlet microchannel length (mm)	X_o	27, 33, 80
Step height (µm)	*S*	200,300,360
Expansion ratio	*ER*	1.5 , 2 , 2.5

Fig.1. Geometry and flow domain of microscale backward-facing step.

2.2 Boundary conditions

The boundary conditions applied for the non-linear partial differential equations (1) of continuity and momentum are:

- At the inlet of the microchannel, the flow velocity is calculated from an imposed Reynolds Red using the following relationship:

$$U = U_{in} = \frac{Re_d . \mu}{\rho . d_h} \qquad (2)$$

- At the walls: u=0, v=0 is used to implement the no-slip requirement.
- At the outlet section flow: $P_{relative} = 0$

3.Numerical method

In general, the method is based on spatial discretization, it combines concepts traditionally associated with finite volume (FVM) and finite element (FEM) methods. The domain is discretized into triangular elements, as for the finite element method (FEM), to which the thermo-physical properties of the flow such as viscosity and density are affected. Interpolation functions are defined on each element, to describe the local variation of speed and pressure. These functions are interpolated linearly to ensure convergence and avoid numerical instabilities, such as the checkerboard problem of the pressure field described by Patankar [26]. Similar to the finite volume method (FVM), the conservation equations are integrated through a control volume to obtain a system of algebraic equations that can be solved for pressure and velocity field determination. The obtained algebraic equations are decoupled using the sequential variable fitting algorithm similar to the well-known SIMPLER (SIMPLE Revised) algorithm, developed by Patankar, but omitting the pressure correction equation. In this procedure the discretized equations for u and v are solved using the iterative Gauss Seidel method with over relaxation SOR (Successive Over-Relaxation). The solving algorithm is repeated several times until the given convergence criterion $\phi^{i+1} - \phi^i / \phi^i \leq 10^{-7}$ reached for all independent variables $\phi = P, u, v$

4. Results and discussion

In this section, we present the results of numerical simulations as well as the interpretation of the different dynamic behaviors observed; of a laminar flow in a microchannel with a singularity, backward facing step. The results are compared, qualitatively and quantitatively, with theoretical correlations, as well as with numerical and experimental results, valid for pipes of conventional size. Note that the classical theory and correlations that describe the flow in a straight macrochannel are given by the following relations [27]:

In fully developed region, the analytical Poiseuille profile is given by:

$$U(y) = -\frac{4U_{\max}}{H^2} y(y-H) = \frac{1}{2\mu}\frac{dP}{dx} y(y-H) \qquad (3)$$

Where;

$$\frac{dP}{dx} = -\frac{8\mu U_{\max}}{H^2} = -\frac{8\mu U_{\max}}{H.h} . \frac{1}{ER} \qquad (4)$$

The maximum velocity value is:

$$U_{\max} = 1.5\overline{U}_{in} \quad (5)$$

The skin friction coefficient: It represents the frictional force that opposes the movement of the fluid.

$$C_f = \frac{dp}{dx}\left[\frac{H}{0.5\rho\overline{U}_{in}}\right] \quad (6)$$

Friction factor: describe the level of friction or resistance to flow in a fluid through a pipe or conduit

$$\lambda = \frac{96}{\mathrm{Re}} \quad (7)$$

Therefore, the Poiseuille number: is a dimensionless quantity that characterizes the flow of viscous fluids through a pipe or conduit

$$Po = C_f * \mathrm{Re} \quad (8)$$

$$P_o = 24 \quad (9)$$

The channel length of entrance is carefully selected to satisfy a full development of the hydrodynamic boundary layer and known as the hydrodynamic entry length. For laminar flow, this entrance length is defined by:

$$Le = C.\mathrm{Re}.D_h \text{ , where } C \in [0.02, 0.06] \quad (10)$$

The singular pressure drop coefficient caused by macro abrupt expansion is evaluated with the following expression:

$$K_e = \frac{\Delta P_s}{0.5\rho\overline{U}_{in}^{\,2}} \quad (11)$$

ΔP_s : Singular pressure losses (see fig.1).

Borda Carnot relation $K_e = (1-\sigma)^2$, σ : area ratio $\equiv \frac{h}{H}$.

4.1 Grid independence study

The simulations were performed using a non-uniform triangular mesh with a higher mesh concentration in close proximity to the walls and the step. A dependency test of the mesh size based on dimensionless separation and reattachment lengths (Xi/S), allowed the adoption of a combination of 29440 elements, which presents a better compromise between the accuracy of the results and the required computational strength (Fig.2(a)-(d)).

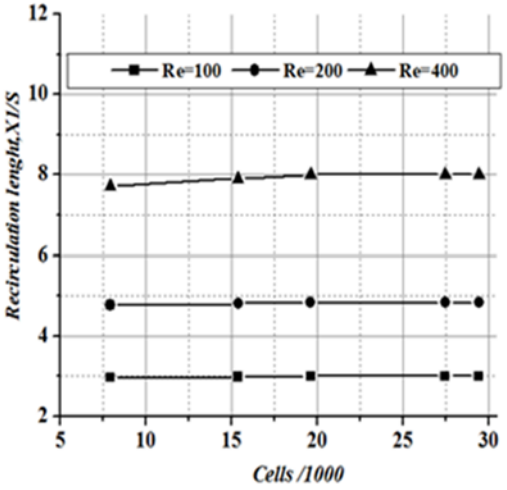

(a)

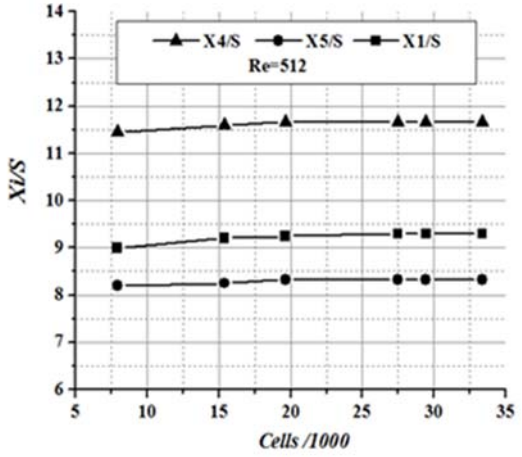

(b)

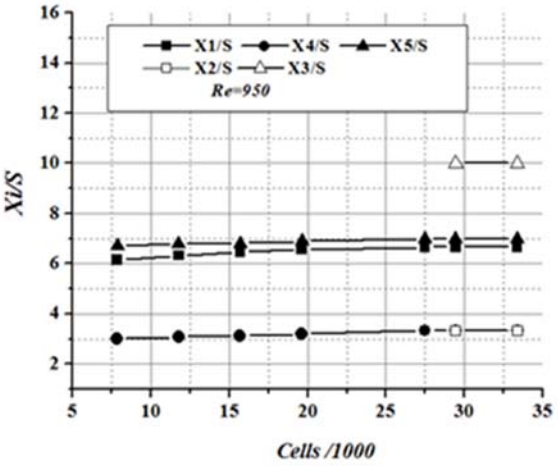

(c)

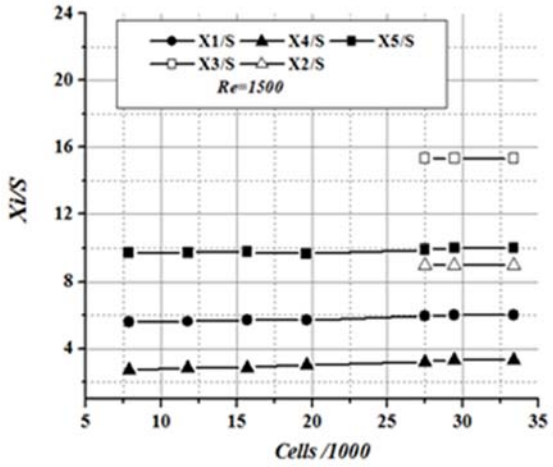

(d)

Fig. 2. Grid independence tests based on detachment and reattachment lengths

4.2 Comparison of simulation results with experimental and numerical results

In this section, we will compare our simulation results with experimental and numerical studies performed in conventional pipes. Only the results corresponding to an expansion ratio ER= 2 are represented (h=300 µm, H=600 µm) with input Reynolds numbers ranging from 0.0001 to 2000. In Fig.3, the streamline patterns for different Reynolds numbers are presented. This figure shows that the flow structure varies with the Reynolds number. For low Reynolds number values (Re_d = 10^{-4}, $10^{-1,}$ and 1), the examination of streamlines does not show any distinction between the upstream and downstream of the singularity. Under these conditions, the flow is known as creeping. The viscosity forces are so predominant and the fluid is attached to the wall of the step and follows its shape without any separation or stagnation points (see Fig.3(a) - (c)). A recirculation zone begins to appear near the step corner at Re_d =5 (Fig.3(d)). The intensity of this recirculation is proportional to the Reynolds number (see Fig.5(e)-(f)) until reaching a threshold value, and then decreases in disproportional way. Beyond Re_d =500 (Fig.3(g)), as a result of the unfavorable pressure gradient caused by the singularity, a secondary vortex will be detected at the upper wall, and begins to growing with the increasing Reynolds number (Fig.3 (h)). At Red=950 (Fig.3(i)), another recirculation zone formed downstream of the step, separate from the primary recirculation zone, and extends for the further simulated Reynolds numbers (see Fig.3 (j)-(k)). These vortical structure obtained within our numerical framework successfully validated the experimental observations of Armaly et al. [10].

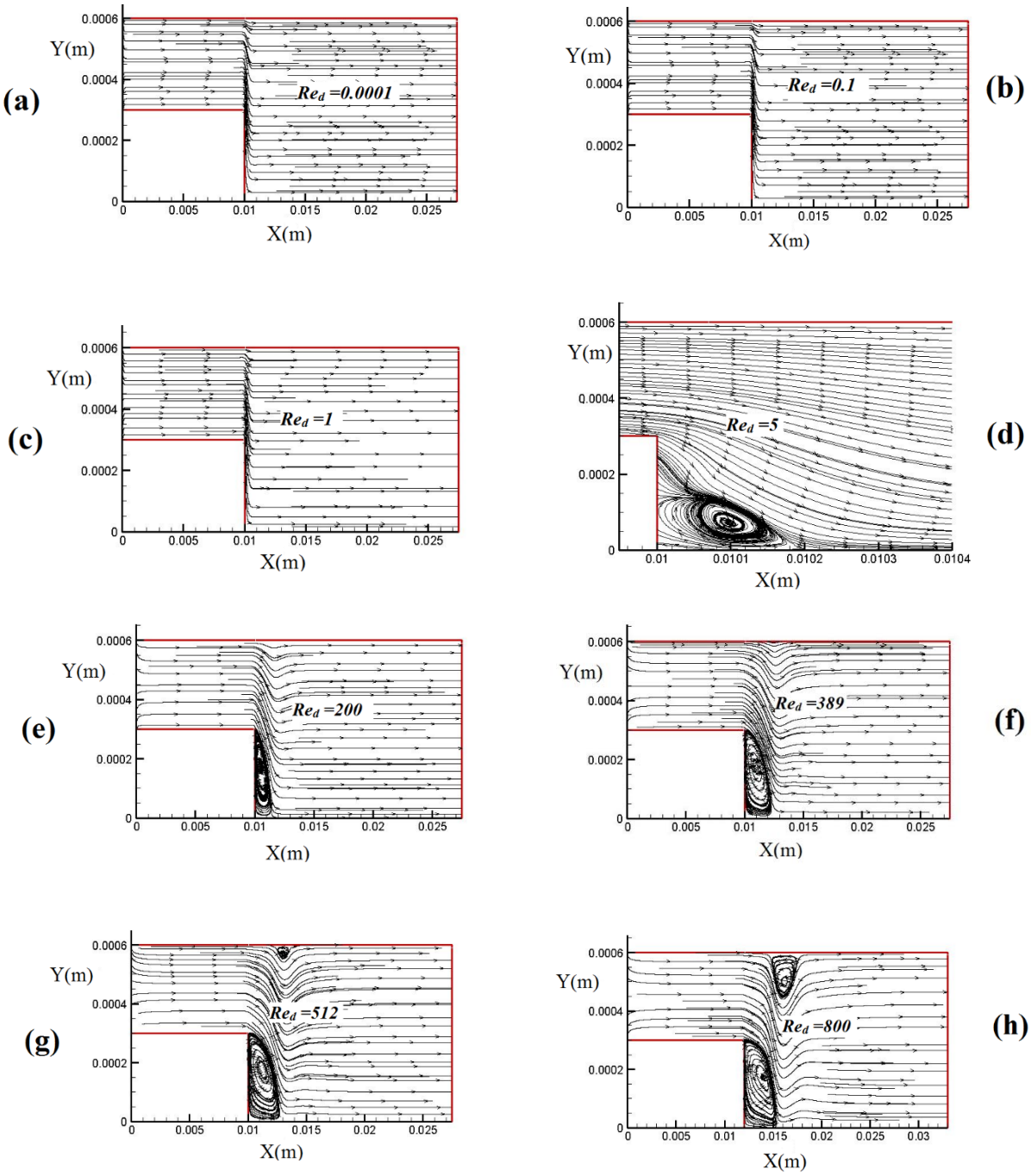

Fig 3. Streamlines Plots at various Reynolds numbers.

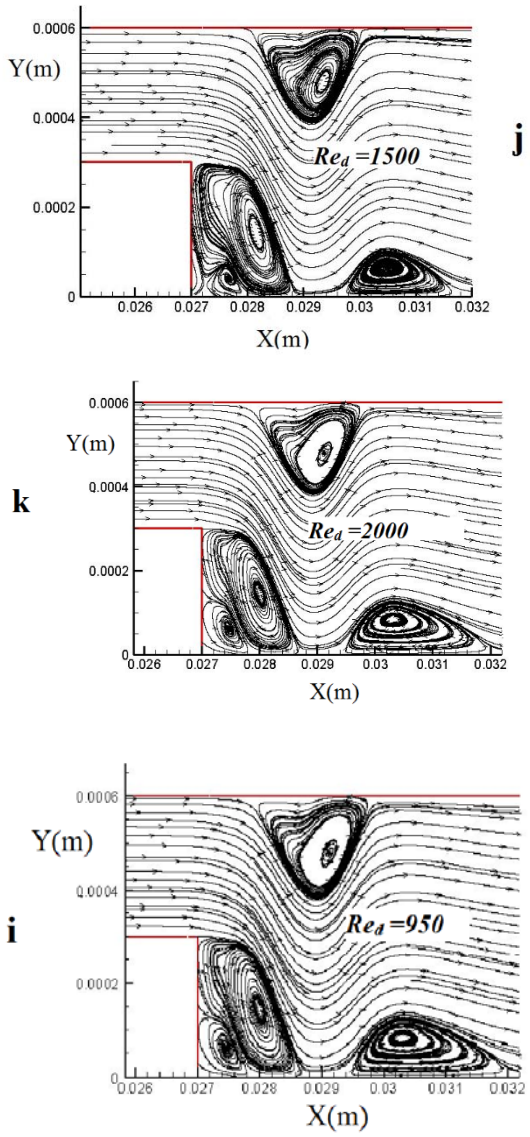

Fig 3. (Continued)

Fig.4 compares our calculated primary recirculation region length X_1/S with the data of Armaly et al. [10] for several Reynolds numbers. A good concordance is noted between the values of the simulations and the experimental values for the laminar regime defined by Reynold number Re_d<500 (Fig.4(a)) _, for which only one vortical structure is formed in the channel. When Re_d exceeds the value of 500, the flow loses its two-dimensional nature with the birth of a second recirculation zone on the upper wall, the numerical values diverge from the measurements and this divergence is accentuated with any increasing Reynolds number. It is visible in (Fig.4(b)) that the transitional regime starts at Re_d =950, a value close to that reported by Armaly et al. [10] (Re_d =1200). It can also be noted that the transient regime is distinguished by the existence of a third recirculation region on the bottom wall and by a decrease in the length of the main recirculation region X1/S with the increasing Reynolds number.

In Table 2, we compare the detachment and re-attachment coordinates thus calculated on the upper and lower walls with the numerical and experimental values provided [10-12], for a Reynolds number value Re_d =800. The results obtained throughout our simulation seem to be close to the experimental and numerical values reported in the macro scale backward-facing step.

Table 3 presents a comparison between the length of the second recirculation zone, X5- X4 obtained experimentally [10] and that determined numerically. It can be clearly seen that the size of the vortex is quite comparable between micro-channel and classical duct.

In Table 2, we compare the detachment and re-attachment coordinates thus calculated on the upper and lower walls with the numerical and experimental values provided [10-12], for a Reynolds number value Re_d =800. The results obtained throughout our simulation seem to be close to the experimental and numerical values reported in the macro scale backward-facing step.

Table 3 presents a comparison between the length of the second recirculation zone, X5- X4 obtained experimentally [10] and that determined numerically. It can be clearly seen that the size of the vortex is quite comparable between micro-channel and classical duct.

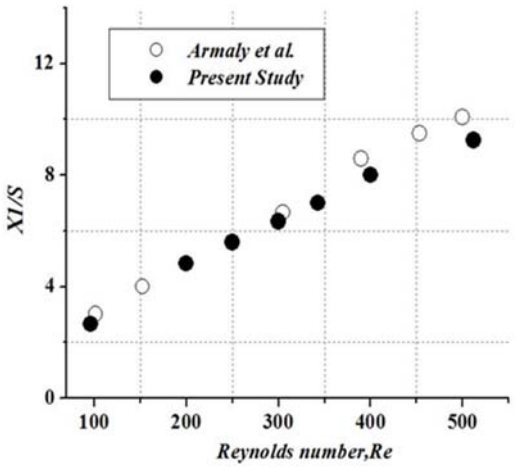

(a)

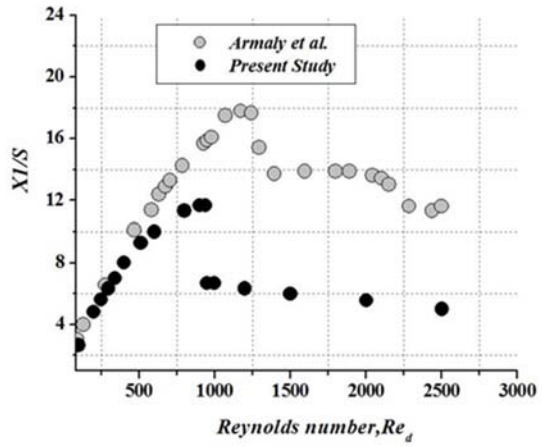

(b)

Fig 4. Variation of X1/S with Reynolds number.

Table 2 Comparison of detachment and Reattachment abscises at Re_d=800.

Present results	Numericals		Experimentals	
CVFEM	Gartling [10]	Lee and Mteescu [12]	Armaly et al. [10]	Lee and Mteescu [12]
X_1/S 1.66	12	12	14	12.94
X_4/S 9.33	10	9.6	11.11	10.6
X_5/S 19	21	20.6	19.33	20.56

Table 3 The length of the second recirculating with some Reynolds numbers.

Reynolds number, Re_d	CVFEM	Experimentals Armaly et al. [10]
	X_5-X_4/S	X_5-X_4/S
512	4	5.5
600	5	6
800	9	8.22
900	10	8.22

The dimensionless velocity profiles at several X/S locations for the following values of Re_d = 100, 389, and 1000 are depicted in Figs ((5) -(7)), respectively. Excellent agreement is found within our numerical predictions and the experimental results for both Re_d = 100 and 389 (see Figs (5(a)-(d)) and (6(a)-(e)). For the case Re_d = 1000, we notice some discrepancies at X/S=10, 14, and 49.59 Fig (7(c)-(e)). This disagreement, also highlighted by Armaly et al. [10], is a consequence of the loss of the two-dimensional character of the experimental flow. Therefore, the two-dimensional assumption using the 2D CVFEM method is no longer suitable for predicting accurately the flow characteristic at this regime.

The evolution of the velocity profiles along the micro-channel for Re_d=100,300 and 500 is schematized on the Fig (8). At the entrance of the micro-channel, we impose a velocity profile 1.0 U_{in}, which begins to develop from a station to another. As $X^+=X/d_h$ increases the velocity at the center of the channel increases and stabilizes at a maximum value 1.48 U_{in}, corresponds *to* the fully developed regime. It can be seen that the value of the max velocity is close to that proposed by classical theory, which provides for a value of U_{max} =1.5U_{in} (Equation 5)**.** When the flow crosses the enlargement, its maximum velocity decreases suddenly, and then increases again gradually until it reaches the analytic fully developed value Uin/2 along the rest of outlet channel.

Fig (9) shows that the hydrodynamic entry length evolves in an increasing and linear manner according to the expression Le/Dh=C.Re_d; with C=0.03, which also agrees with the macroscale theory as in equation 10.

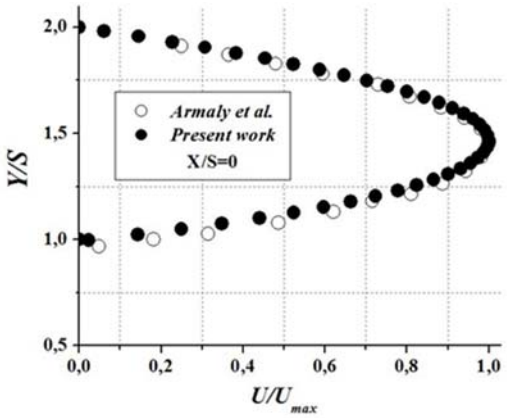

(a)

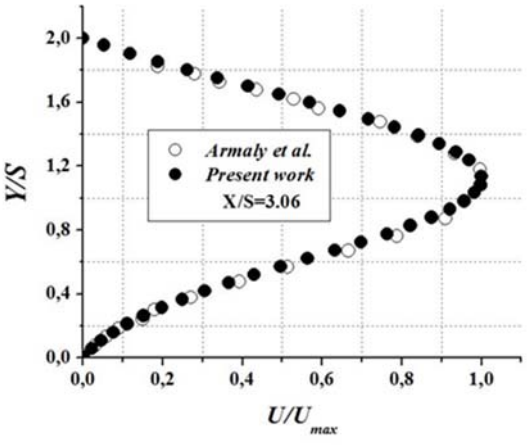

(b)

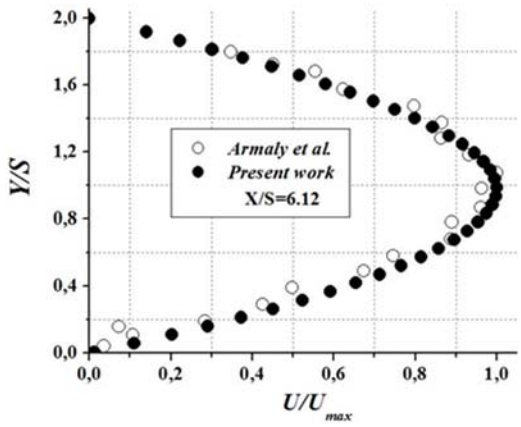

(c)

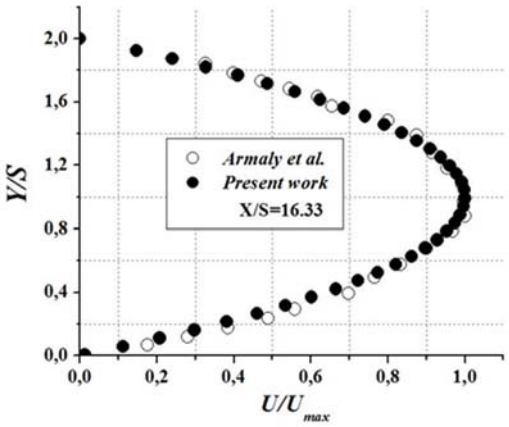

(d)

Fig 5. Velocity profiles at different sections downstream of the step for Re_d =100.

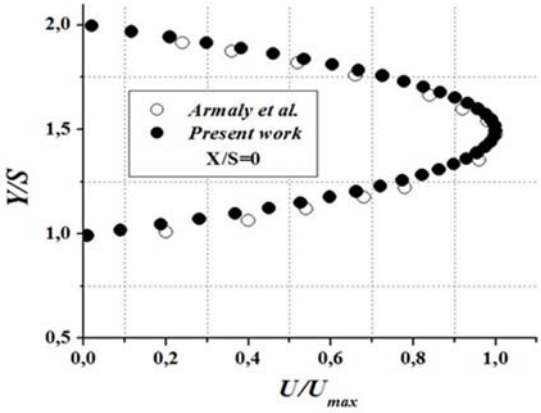

(a)

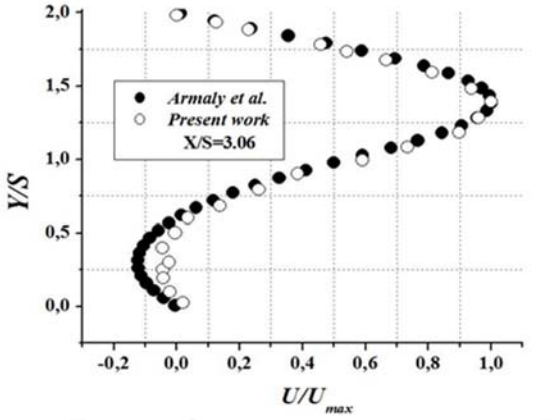

(b)

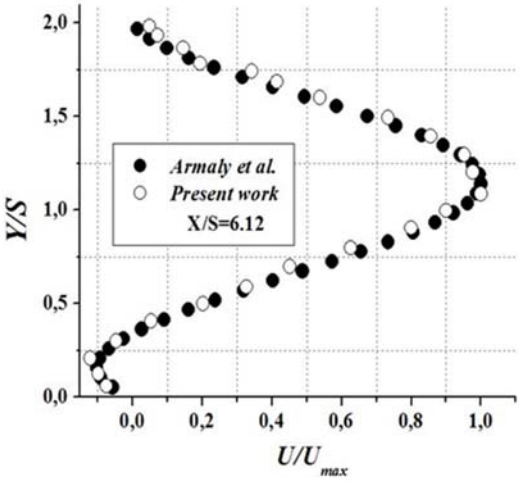

(c)

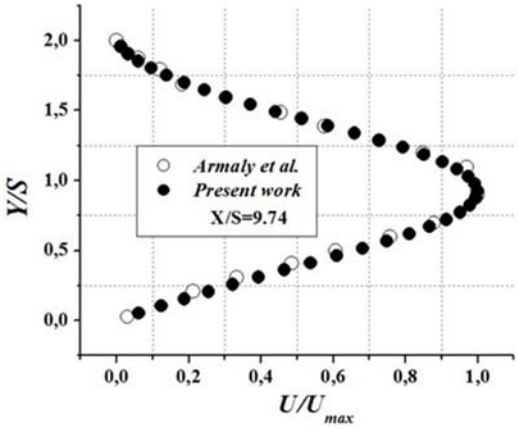

(d)

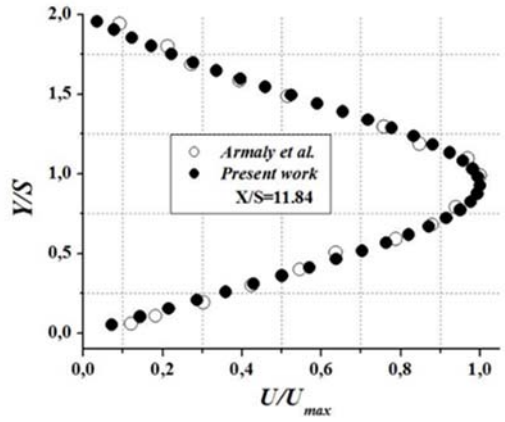

(e)

Fig 6. Velocity profiles at different sections downstream of the step for Red =389.

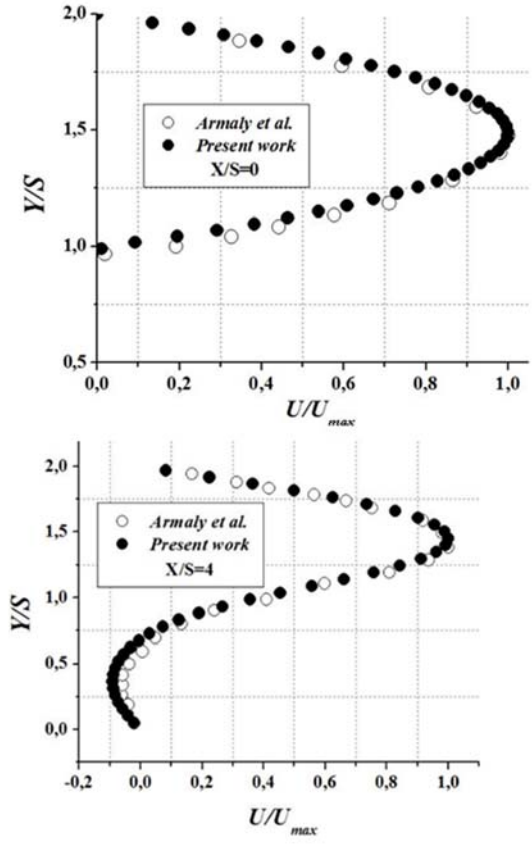

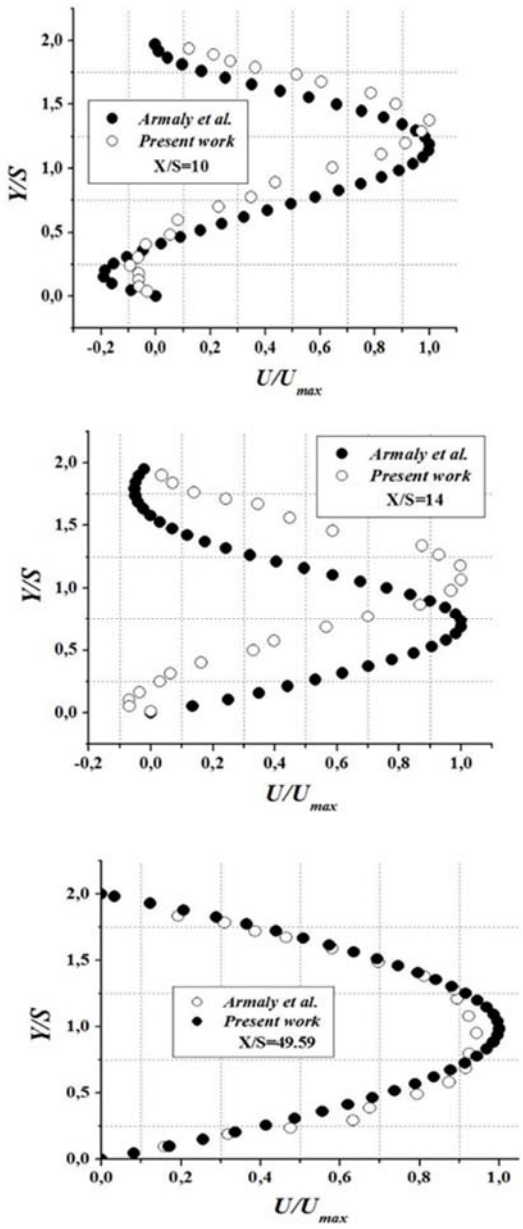

Fig 7. Velocity profiles at different at sections downstream of the step for Red =1000.

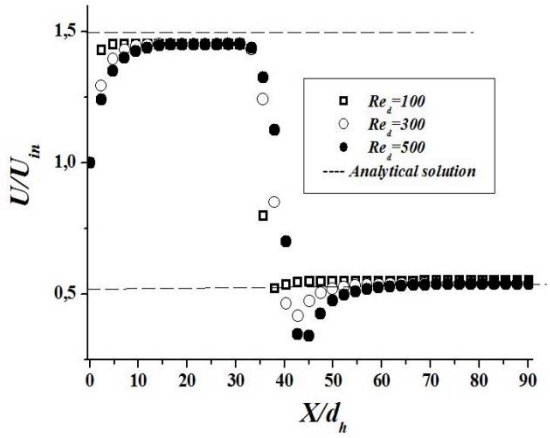

Fig 8. Dimensionless centreline axial velocity at various Reynolds numbers.

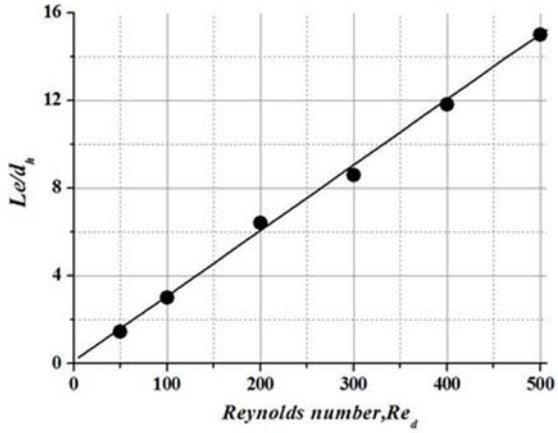

Fig 9. Variation of hydrodynamic entry length with Reynolds number in small channel.

4.3 Comparison of simulation results with classical theory:

In this section, the simulation results are compared with classical correlations established in the case of conventional size pipes, over a Reynolds range where the flow keeps its two-dimensional character, Re_d<500. The parameters analysed, pressure drop, the global friction coefficient at the wall and the singular pressure drop coefficient.

In Fig .10. a, the static pressure increases sharply from the step angle until it reaches its maximum value at detachment point X1, end of the recirculation zone, and then decreases linearly until it reaches 0 Pascal, value of the relative pressure imposed at the exit of microchannel. An increase in the Reynolds number is accompanied by an increase in the pressure peak value.

In table 4**,** a good agreement is noted between the calculated pressure gradient values and those classically encountered at conventional scales (Equation 4)**,** suggesting that no scale effects.

The variation of the skin friction coefficient and Poiseuille number as a function of the Reynolds number is shown in Fig 10(b) and 10(c), respectively. It can be seen that all the curves have the same trend. They are decreasing in nature in the recirculation zone, then increase, outside of this zone, to stabilize at a maximum value along the rest of the microchannel, indicating that the flow is hydrodynamically fully developed. Good agreement is noted between the calculated values and those encountered at conventional scales for fully developed steady-state laminar flow. Moreover, the minimum value of the skin friction coefficient and Poiseuille number, in the recirculation zone, decreases with increasing Reynolds number, and its position moves downstream of the step. Also, outside the recirculation zone, we notice that for higher Reynolds number values, C_f is smaller (Equation 6)**.** This is explained by the fact that the increase in inertial forces accelerates the movement of particles and overcome the effect of viscous forces.

Fig.10(d) represents a comparison between the friction factor obtained numerically and that calculated analytically from the equation $\lambda = 96/Re_d$. The simulation results seem to be in good agreement with the values of the equation ($\lambda = 96/Re_d$) established for conventional channels. This result only confirms the similarity of the laws in the case of a laminar regime.

Fig.11 compares the numerical loss coefficients with the predictions of the **Borda-Carnot** relation, i.e., $Ke = (1 - \sigma)^2$. For Re_d >200, the results indicate higher values than the Borda-Carnot relation, as Ke correlates well with the value Ke = 0.32. For $Re_d \leq 200$, Ke can be expressed as a function of Re_d via the following correlation:

$Ke = a + bRe_d + cRe_d^2$ with, a=0,03252, b=0,00169, c= -2,27652E-6

Fig 12(a) and 12(b) show the variation of the static pressure gradient and the Poiseuille

number downstream of the step for different expansion ratios.

All curves have the same trend and converge to the analytical solution when the flow is fully developed (Equation 4 and 9). The values of the pressure gradient and Poiseuille number decrease from 0 at the wall of the step to a minimum value at the point of reattachment. The abscissa of this minimum moves downstream of the channel with increasing expansion ratio. This indicates that the size of the recirculation zone increases with increasing expansion ratio.

Table 5. Comparison of numerical and theoretical pressure gradient.

Reynolds numbers, R_{ed}	dP/dX [Pas/m] (numeric)	dP/dX [Pas/m] (Theory)
100	-665.7	-662.84
300	-2375.8	-2373.22
500	-3559	-3542.53

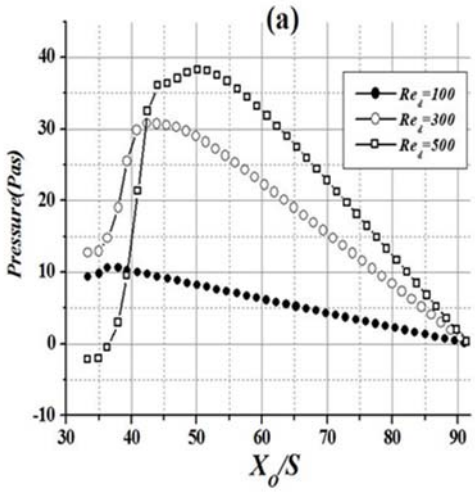

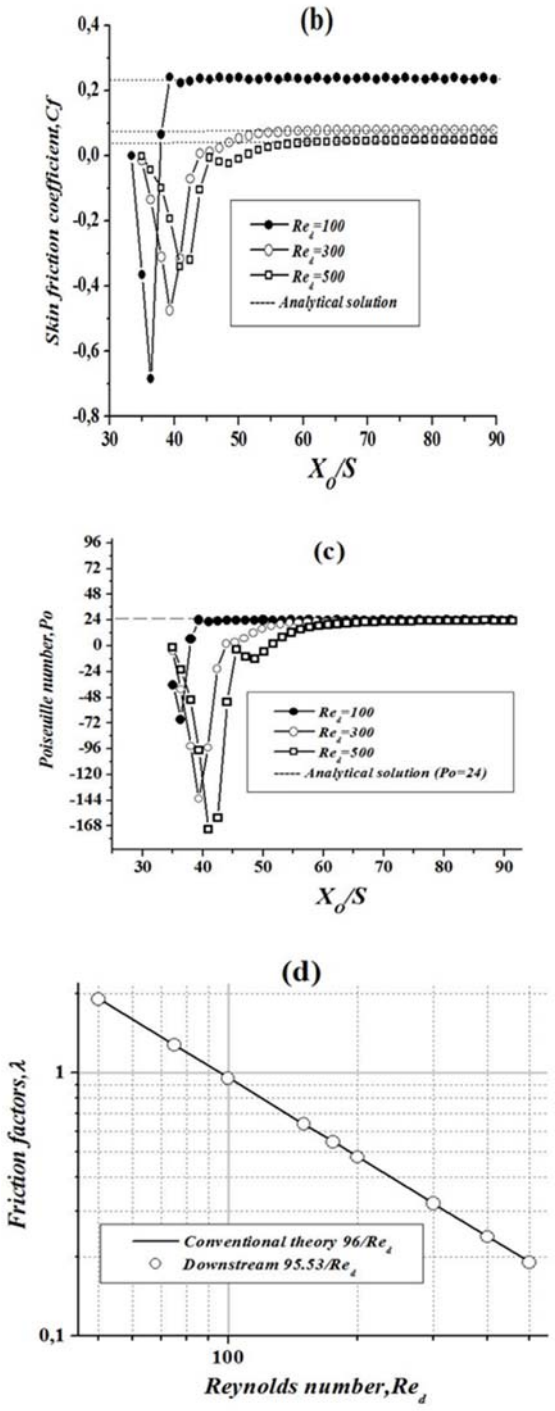

Fig 10. Flow parameters downstream of the step (ER=2) (a) pressure, (b) skin friction coefficient, (c) Poiseuille number, (d) Friction factors.

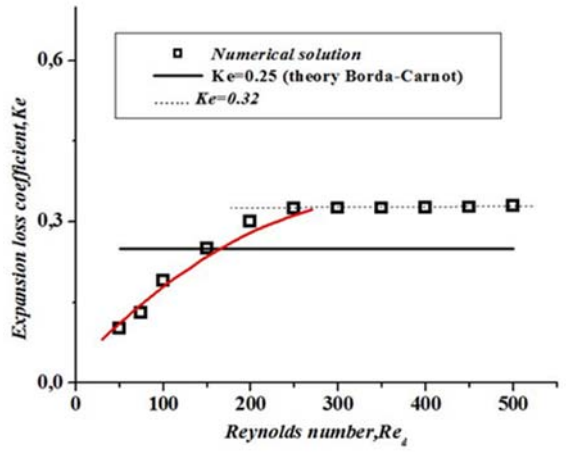

Fig 11. Evolution of expansion loss coefficient according to the Reynolds number (ER=2).

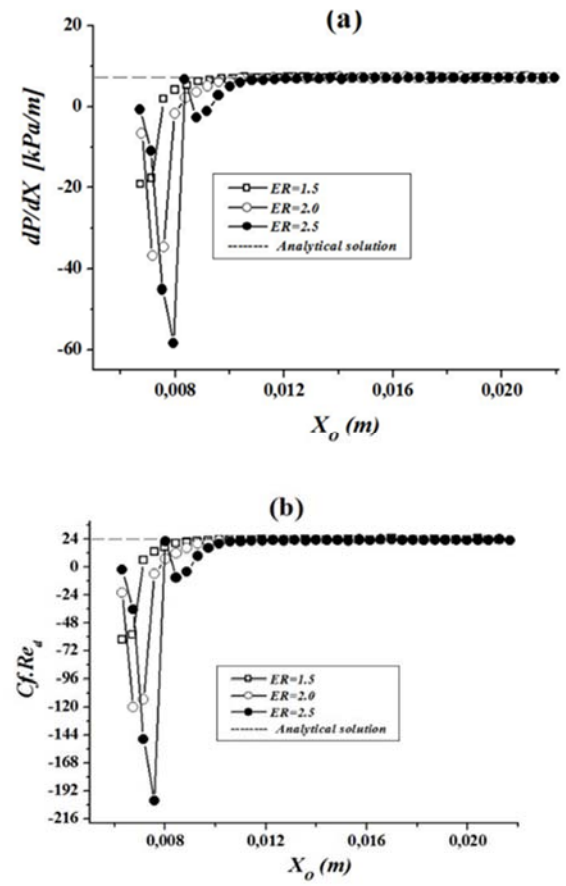

Fig 12. Variations of (a) static pressure gradient and (b) Poiseuille number at different expansion ratios downstream of the step for Re_d =300.

5.Conclusions

In the present study, we studied numerically a two-dimensional laminar flow in a microchannel with a backward step. The numerical simulations were performed using a code developed in Fortran language based on the combined Control Volume Finite Element Method (CVFEM). We analyzed the effect of Reynolds number and expansion ratio on the dynamic behavior of the flow. The purpose was to verify the applicability of classical laws and correlations of hydrodynamics at microscale.

For an expansion ratio ER=2 and over a Reynolds range that extends from 0.0001 to 2500, the numerical results show that the structure of the flow pattern seems in good agreement with the experimental observations reported in macroscale backward-facing step by Armaly et al. There is a formation of three recirculating regions behind the step, in both laminar and transitional regime, two at the lower wall and another at the upper wall. Also, the flow reattachment length and the velocity profiles successfully validate the experimental results in the laminar range Red≤500 when there is only one vortex. However, a deviation from the measurements is noted for Reynolds higher than 500, with the appearance of a second recirculation zone on the upper wall, and this disagreement increases with increasing Reynolds number. This is due to the fact that the flow loses its two-dimensional character. In addition, the flow parameters at the downstream of the singularity, in terms of axial velocity, pressure drop, skin friction coefficient and Poiseuille number, agree well, qualitatively and quantitatively, with the theoretical correlations, and demonstrates quite clearly that the laws of hydrodynamics remain valid for Red≤500. The results also show that the loss coefficients were significantly higher than what is expected in conventional macro systems for Red >200. For lower values of Reynolds, however, the loss coefficient varied with Red. For the rest of the work, we performed numerical simulations on two other microchannels of expansion ratio ER=1.5 and 2.5. The aim was to detect possible differences in the flow behavior. We are particularly interested in the evolution of the pressure gradient and Poiseuille number. The results confirm that the hydrodynamic

characteristics remain consistent with the classical correlations.

The numerical technique presented in this paper can be successfully employed to calculate the flow field in microscale geometries. At these scales, a technological rupture occurs and the traditional methods of measurement and machining become inappropriate.

References

[1] R J. Singh and T B. Gohil, Numerical Analysis of Unsteady Natural Convection Flow and Heat Transfer in the Existence of Lorentz Force in Suddenly Expanded Cavity Using Open FOAM. J. Thermal Science (2020); 29: 1513–1530.

[2] H .Binghuan, L .Haiwang, and X. Tiantong . Experimental investigation of the flow and heat transfer performance in micro-channel heat exchangers with cavities. Int J Heat and Mass Transfer (2020);159 : 120075.

[3] Z .Dongwei, F .Luotong , G .Jian , Chao Sh and T .Songzhen ,Investigation on the heat transfer and energy-saving performance of microchannel with cavities and extended surface. Int J Heat and Mass Transfer (2022); 189 : 122712.

[4] H .Tingbo and X. Danmin, Pressure drop and heat transfer performance of microchannel heat exchangers with elliptical concave cavities. Applied Thermal Engineering (2023); 218: 119351.

[5] E. Jiaqiang, M Tian, Jingwei Ch, Weiwei Wu, Z. Xiaohuan, Z .Bin and P.Qingguo, Effect analysis on performance enhancement of a hydrogen/air non-premixed micro combustor with sudden expansion and contraction structure. Energy journal 2021; 230: 120727

[6] Yan T J E , Jingwei Ch G, Liao F Zh and Jintao L. Investigation on combustion characteristics and thermal performance of a three rearward-step structure micro combustor fueled by premixed hydrogen/air. Renewable Energy 2022; 186: 86-504.

[7] Evan L, Stephen L, Kevin L, Hongzhou X and Michael F. The effect of diffuser shape for film cooling holes with constant expansion angles and area ratio. Proceedings of the ASME, Turbomachinery technical conference and exposition Rotterdam, Netherlands 2022.

[8] Andrea N and Paolo G. The Role of Turbine Operating Conditions on Combustor Turbine Interaction Change in Expansion Ratio. ASME 2022, J Turbomachinery 2023; 145: 5 .

[9] Ramanathan S, Thansekhar MR, P RajeshKanna and Prem G. A new method of acquiring perquisites of recirculation and vortex flow in sudden expansion solar water collector using vortex generator to augment heat transfer. Int J Thermal Science 2022; 153: 106346

[10] Armaly B F, Durst F, Pereira J C F and Schonung B. Experimental and theoretical investigation of backward-facing step flow. J Fluid Mechanic 1983; 127: 473–496.

[11] Gartling D K. A test problem for outflow boundary conditions-flow over a backward-facing step . Int J Numerical Method in Fluids 1990; 11: 953– 967.

[12] Lee T and Mateescu D. Experimental and numerical investigation of 2D backward facing step flow. J Fluids and Structure 1998; 12: 703–716.

[13] Hammad K J, Otugen M Vand Arik E B. A PIV study of the laminar axi- symmetric sudden expansion flow. Experiments in Fluids 1999; 26: 266-272.

[14] Lima. R C, Andrade C R. and Zaparoli E L. Numerical study of three recirculation zones in the unilateral sudden expansion flow. Int Comm Heat and Mass Transfer 2008; 35: 1053–1060

[15] Roy V, Majumder S and Sanyal D. Analysis of the Turbulent fluid flow in an axi symmetric Sudden Expansion. Int J Engineering Science and Technology 2010; 2 :1569-1574.

[16] Sudipta R, Nirmalendu B, Prokash C and Roy. Investigation of Newtonian Fluid Flow through a Two Dimensional Sudden Expansion and Sudden Contraction Flow Passage. Int J Engineering Research and Development 2012; 1(12): 01-09.

[17] Nowruzi H, Salman Nourazar S and Ghassemi H. On the Instability of Two Dimensional Backward-Facing Step Flow using Energy Gradient Method. J Applied Fluid Mechanics 2018; 11: 41-256.

[18] Toufik Chalfi Y and Ghiaasiaan S M. Pressure drop caused by flow area changes in capillaries under low flow conditions. Int J of Multiphase Flow 2008; 34(1) :2–12.

[19] Abdelall F F, Hahn G, Ghiaasiaan S M and Abdel Khalil S I. Pressure drop caused by abrupt flow area changes in small channels. Exp Ther and Fluid Science 2005; 29(4): 425-434.

[20] Hang G, Ling W, Jian YU, Fang Y E, Chongfang M A and Zhuo L I. Local resistance of fluid flow across sudden contraction in small channels. Frontiers of Energy and Power Engineering 2010; 4: 149-154.

[21] Sepideh K, Navid B and John R T. Sudden expansions in circular microchannels: flow dynamics and pressure drop. Microfluidics and Nanofluidics 2014; 17: 561–572

[22] Hassnia. H, Lioua K, Kaouther G, Chemseddine M, Ahmed K H and Mohamed N B Numerical

study of heat transfer and flow structure over a microscale backstep. Alexandria Engineering journal. 2021; 60(3): 2759–2768.

[23] Saabas H J and Baliga B R. Co-located equal-order control-volume finite element method for multidimensional incompressible fluid flow. Numerical Heat Transfer 1994; 26(4): 381–407.

[24] Luu D T, Christian M and Arezki S. A stable second order mass weighted upwind scheme for unstructured meshes. Int J Numerical Methods in Fluids 2006; 51(7): 749-771.

[25] Baliga B R and Patankar S V. A New Finite-Element Formulation for Convection Diffusion Problems. Numerical Heat Transfer 1980; 3 :393-409.

[26] Patankar V. Numerical heat transfer and fluid flow. New York, USA: Hemisphere, 1980.

[27] White F M. Fluid Mechanics. 8th ed. McGraw-Hill Education, 2016